Engineering and Technology Journal 40 (10) (2022) 1295-1306

Engineering and Technology Journal
Journal homepage: https://etj.uotechnology.edu.iq

Images Enhancement Based on a New Multi-Dimensional Fractal Created by Rectangular Function

Rabab F. Abbas*

Computer Science Dept, University of Technology - Iraq, Alsina'a Street, 10066 Baghdad, Iraq.
*Corresponding author Email: mailto:rabab.f.abbas@uotechnology.edu.iq

HIGHLIGHTS

- New Multi-Dimensional Fractal was introduced to improve and enhance the images.
- Different images with low gray levels were enhanced by applying the suggested enhancement model.
- The improvement brought a 97% rate in PNSR and a 95% rate in RMSD.

ARTICLE INFO

Handling editor: Rana F. Ghani

Keywords:
multi-dimensional fractal; fractal; rectangle function ;image enhancement; mask.

ABSTRACT

Digital image processing is a field that is included in many journals due to its importance and the fact that it facilitates the achievement of many scientific and engineering applications worldwide. This specialization is linked with other disciplines, whether medical, engineering, sports, and others, as it facilitates the completion of applications quickly and efficiently. Researchers have discovered and garnered notice as a promising analytic tool in image processing using the idea of fractal dimension. In this effort, a new Multi-Dimensional Fractal (MDF) in view of the rectangle function was introduced a. As an application, the MDF to improve and enhance the images was employed, and found that there is a connection between MDF and image processing, where the self-similarity property, for example, is one of several features in the new definition. Other properties are discussed in the sequel, including image noise reduction. The presence of noise is responsible for properly operating these images in various applications. Several academics have created and applied a strategy for minimizing noise in features multiplicatively throughout the last several years. The outcomes reveal that the proposed strategy is successful. The method is based on the definition of the rectangular function (the elementary component of all digital signals, videos, and images), where this function indicates a rectangular-formed rhythm that is concentrated at the origin. For example, the suggested process received a rate of 97% for PNSR and 95% for RMSD.

1. Introduction

The use of fractional and fractal notions has grown in popularity over the last twenty years due to their benefits. Almost every study found that reordering these two principles resulted in a significant increase in image processing. Image noise is a significant issue in all image investigations, such as segmentation, texture examination, and image removal. Denoising is the most common stage in image processing. Reduced noise in image multiplicative (DNM) has recently been suggested. The exploration of Commonsensical Imaging Assemblies (CIA) [1, 2]. Employing synthetic aperture radar, laser, and ultrasound is being driven by DNM imitators. The normal stabilizer noise assembly is insufficient for catching such images because of the commonsense setup of these image success operations. DNM models provide excellent CIA score explanations. DNM formed using partial and ordinary diffusion equations, variation techniques, slope operational methodology, fractional entropy type Tsallis entropy, and updated fractional calculus, including conformable fractional calculus, have all shown improved performance [3-6].

In all areas, including computer sciences, the fractal and fractional operators (differential and integral) are concisely proposed in image processing [7-11]. It's for medical MRI improvement [12] and is suggested in feature treatment. Furthermore, noise refers to any unwanted signal (note that multiplicative noise is defined as an unrequited arbitrary signal multiplied into a specific connected signal during processing) that perverts digital images, primarily through feature realization, which is the process of converting an optical image into continuous electrical signals. To clarify the challenges in constructing an X-ray feature, some research related to numerical image processing and statistical analysis of X-ray images is suggested [13]. In [14,

http://doi.org/10.30684/etj.2022.134235.1229
Received 10 June 2022; Accepted 12 August 2022; Available online 07 September 2022
2412-0758/University of Technology-Iraq, Baghdad, Iraq

15], the authors suggest a well-organized differential box-counting approach for calculating the fractal dimension of feature enhancement. The study of polymer images [16] has seen more applications of FD. Furthermore, a sort of fractal known as the quantum fractal (also known as the Jackson fractal) has recently been utilized to assess medical photographs [17, 18, 19].

Researching consistent imaging arrangements such as sonar, ultrasound, laser, and radar requires multiplicative noise images. In light of the systematic Gaussian preservative noise issue, these photos explain two additional films of difficulty: first, the noise is multiplied by the original image; second, the noise is not Gaussian [20]. In [21], the researchers investigated a theoretical investigation for non-autonomous stochastic fractional equations generated by multiplicative noise, with the fractal dimension bounding in the unit interval $I = (0,1)$. Researchers in [22, 23] provide fractal analyses and surface organization in authentication and identification protocols. A medicinal picture verification technique is accomplished in the researchers' attempt in [24] related to wavelet reestablishment and fractal dimension analysis. The images are eliminated, and a fractal property is formed as the verification image of the pictures when rendering to the singularity of the fractal dimension of the block data [25-39].

In this work, a new approach based on a central kind of MDF and the rectangular function was proposed in this investigation. MDF's advantages include using a multi-dimensional formula in its creation, which may be applied to analyzing complicated systems such as images. Four masks are proposed for x and y orders intended to predict the predicted structures of MDF windows. For capacity, different strainers are used. The investigation revealed that skilled filtering has a higher score than several current fractional and fractal filters.

Following are the stages: The approach to be employed in the recommended strategy is discussed in Section 2. The new MDF, generic window, and fractional mask are all part of it. Section 3 discusses the use of the recommended approach MDF in image enhancement. Finally, section 4 will include the conclusions, last comments, and future works.

1.1 Related Works

This section presents a list of related works using the method of rectangle function in image processing. The smooth rectangle function is considered in the work of Boukharouba [40] to design a filter in image processing. Yang et al. [41] utilized image processing approaches to investigate hydrodynamic features in a rectangular function. Training data is also investigated by Bargsten and Schlaefer [42] with the help of the rectangle function. He et al. [43] improved the edge extraction algorithm via the rectangle function. Meng et al. [44] designed a mathematical model for heterogeneous material based on digital image processing by employing the rectangle function. Ferreira et al. [45] approximated the rectangle function to model color image processing. The multi-dimensional fractal approach in this study by using the rectangle function was modified. The new technology is used to improve images as a software application. Recently, the multi-dimensional fractal has been indicated in image processing covering many factors in this area, such as the remote sensing images [46], the similarity of images [47], enhanced images [48], and classification of images [49] and optical images [50].

2. The Proposed Method

The following subsections are included in this section:

2.1 Multi-Dimensional Fractal (Mdf)

Dimension (size) box-totaling: The box-counting mod [25] for fractal dimension is the most casual and often used method in nonfiction. Using a binarized image of the retinal tree as a starting point, the image was covered with a network of side-length boxes and calculated the number of boxes, which included a portion of the tree. Now minimizing the casing, more information about the tree was extracted. The structure formulates the box count as a function of the box-totaling size by letting $N(wp)$ be the box-count as a function of the box-totaling size [26, 27].

$$ð_{\flat} = \lim_{\flat \to 0} \left(\frac{\log(N(\flat))}{\log(1/\flat)} \right), \tag{1}$$

Where $\flat$ denotes the grid cell size (a place-designated neuron) and $N(\flat)$ the number of cells.

The technique for determining the box-totaling dimension is computed similarly in information theory (entropy theory) and by employing values of the item, as follows: [28, 29]

$$ð_{\flat}(\Xi) = \lim_{\flat \to 0} \left(\frac{\sum_{k=1}^{N(\flat)} p_k \log(p_k)}{\log(1/\flat)} \right), \tag{2}$$

where Ξ is the entropy, $N(\flat)$ is the overall sum of boxes that contains a portion of the tree and

$$p_k = \frac{\nu_k}{\mathrm{C}} \in (0,1) \tag{3}$$

is the quantity of retinal tree enclosed in the k-the box; the total of pixels in k-the box is ν_k, and the sum of pixels in the tree is C. Finally, the correlation integral, approximated by the summation formal, is used to build a correlation structure [30].

$$ð_{♭}(ℵ) = \lim_{♭ \to 0} \left(\frac{\log \mho(♭)}{\log(♭)}\right), \tag{4}$$

where

$$\mho(♭) = \frac{1}{N^2(♭)} \left(\sum_{k,l=1,k\neq l}^{N(♭)} \hbar(♭ - \| \chi_k - \chi_l \|)\right) \tag{5}$$

$$\approx \sum_{k=1}^{N(♭)} p_k^2,$$

Where $ℵ$ is the correlation, $\hbar$ indicates the Heaviside function, and the number of tree pixel pairs with the distance between them is less than $♭$. Finally, the extended structure (multi-fractal structures) is considered by the formal for a real number $q \in \mathbb{R}\backslash\{1\}$ [31].

$$ð_{♭}(q) = \frac{1}{1-q} \lim_{♭ \to 0} \left(\frac{\log(\Upsilon(q, ♭))}{\log(1/♭)}\right), \tag{6}$$

where

$$\Upsilon(q, ♭) = \sum_{k=1}^{N(♭)} p_k^q.$$

Confirm that all of the above MDF fulfill the inequality below, which is a highly useful pattern for computing fractal dimensions in rehearsal [32, 33]

$$ð_0 \geq ð_1 \geq, \cdots, \geq ð_N.$$

Each of these MDFs was used to explain the overall dynamical, topological, and geometric properties of a given arrangement, including the higher order extensions $ð_{♭}(q)$. However, understanding how these assets evolve at various dimensions is crucial [34].

2.2 MDF Defining By RF

The rectangular function is formulated by the structure:

$$\Re(x) = \begin{cases} 0, & \text{if} |x| > \frac{1}{2} \\ \frac{1}{2}, & \text{if} |x| = \frac{1}{2} \\ 1, & \text{if} |x| < \frac{1}{2}. \end{cases}$$

A limit of a rational function can also be used to represent the rectangle function.

$$\Re(x) = \lim_{n \to \infty, n \in Z)} \frac{1}{(2x)^{2n} + 1}.$$

New formulate MDF utilizing RF was proceeded. The correlation structure (6) implies that:

$$ð_{♭}(ℵ)_{\Re} = \lim_{♭ \to 0} \left(\frac{\log \mho(♭)}{\log(♭)}\right), \tag{7}$$

Where:

$$\mho(♭) = \frac{1}{N^2(♭)} \left(\sum_{k,l=1,k\neq l}^{N(♭)} \Re(♭ - \| \chi_k - \chi_l \|)\right)$$

$$\approx \sum_{k=1}^{N(♭)} p_k^2.$$

Using the accumulated formula to get the generalized structure:

$$ð_{♭}(q)|_{\Re} = \frac{1}{1-q} \lim_{♭ \to 0} \left(\frac{\log \Re(q, ♭))}{\log(1/♭)}\right), \tag{8}$$

Where:

$$\Re(q, \flat) = \sum_{k=1}^{N(\flat)} p_k^q$$

Where:

$$p_k := \frac{1}{(2\flat)^{2n} + 1}, \quad \flat \geq 1.$$

3. Image Denoising Method

In digital images, the Image Denoising Method (IDM) has various effects, some of which are almost invisible. Image denoising aims to yield a fresh feature with less noise, i.e., a feature closer to noise-free. Pixel-based picture filtering and patch-based filtering are the two basic ways that IDMs use to recognize images. The first technique uses a contiguity functional (juxtaposition) that operates on a single pixel and depends on its three-dimensional neighboring pixels inside a kernel. The second category employs blocks of identical patches that are then operated definitively to transmit an estimate of the main pixel values based on comparable bits within an observed window. This approach focuses on the work image's termination, and similarity among the most common portions see Figure1 and Figure 2.

The problem of image denoising is designed mathematically as follows:

$$\Im_{noisy} = \Im_{original} + \iota, \tag{9}$$

where $\Im_{noisy}$ presents the figured noisy image, $\Im_{original}$ indicates the novel (main) image, and ι is the additive white Gaussian noise (AWGN) with standard deviation. Many methods, including median absolute deviation [36], block-based approximation [37], and conventional module analysis cited3, are used to calculate AWGN in applied presentations. The noise reduction goal is to minimize the loss of creative elements while improving the signal-to-noise ratio (SNR). According to polls [39], the basic standards for image denoising are: smooth areas must remain planar, edges must be threatened without blurring, textures must be preserved, and new objects must not be stopped.

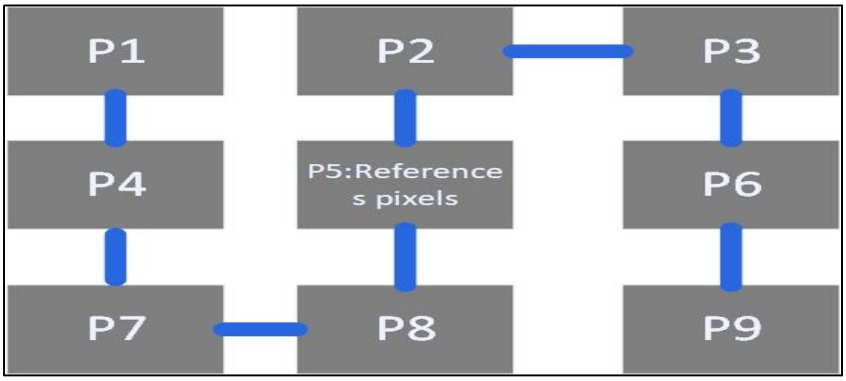

Figure 1: A contiguity operation is the first category in IDM

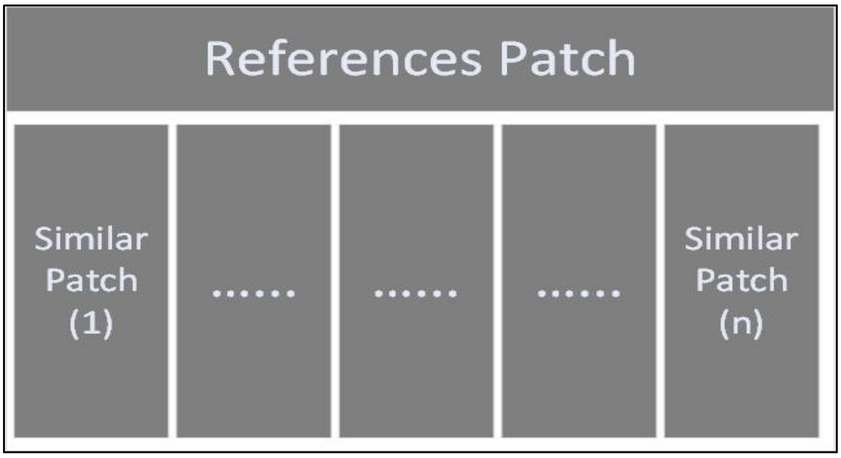

Figure 2: Blocks of comparable patches are used in the second category of IDM

4. Algorithm

Eq.s(7) and (8) are used in this method. Eq.(7) shows a 1-D parametric conclusion with the parameter $\flat$, whereas Eq. (8) shows a 2D one with the parameters $\flat$ and q. To improve the noisy image will use both of these equations to get the indicated improved picture by using Eq.s(7) and (8) together

$$\Im_{noisy} = \Im_{original} * U_{3\times 3}[\eth_{\flat}] \tag{10}$$

and

$$\Im_{noisy} = \Im_{original} * U_{3\times 3}[\eth_{\flat}(q)], \tag{11}$$

respectively, where $*$ is the convolution product and $U_{3\times 3}$ represents the window mask of size 3×3. In this study, different masks are organized as follows, using (7)

$$U_{0^\circ} = \begin{bmatrix} 0 & 0 & 0 \\ \eth_{\flat}(2,1) & \eth_{\flat}(2,2) & \eth_{\flat}(2,3) \\ 0 & 0 & 0 \end{bmatrix}, U_{45^\circ} = \begin{bmatrix} 0 & 0 & \eth_{\flat}(1,3) \\ 0 & \eth_{\flat}(2,2) & 0 \\ \eth_{\flat}(3,1) & 0 & 0 \end{bmatrix} \tag{12}$$

$$U_{90^\circ} = \begin{bmatrix} 0 & \eth_{\flat}(1,2) & 0 \\ 0 & \eth_{\flat}(2,2) & 0 \\ 0 & \eth_{\flat}(3,2) & 0 \end{bmatrix}, U_{135^\circ} = \begin{bmatrix} \eth_{\flat}(1,1) & 0 & 0 \\ 0 & \eth_{\flat}(2,2) & 0 \\ 0 & 0 & \eth_{\flat}(3,3) \end{bmatrix}. \tag{13}$$

Similarly, by using (8) and $\eth_{\flat}(q)$, then the following structures are obtained:

$$\Upsilon_{0^\circ} = \begin{bmatrix} 0 & 0 & 0 \\ \eth_{\flat}(q)(2,1) & \eth_{\flat}(q)(2,2) & \eth_{\flat}(q)(2,3) \\ 0 & 0 & 0 \end{bmatrix}, \tag{14}$$

$$\Upsilon_{45^\circ} = \begin{bmatrix} 0 & 0 & \eth_{\flat}(q)(1,3) \\ 0 & \eth_{\flat}(q)(2,2) & 0 \\ \eth_{\flat}(q)(3,1) & 0 & 0 \end{bmatrix} \tag{15}$$

$$\Upsilon_{90^\circ} = \begin{bmatrix} 0 & \eth_{\flat}(q)(1,2) & 0 \\ 0 & \eth_{\flat}(q)(2,2) & 0 \\ 0 & \eth_{\flat}(q)(3,2) & 0 \end{bmatrix}, \tag{16}$$

$$\Upsilon_{135^\circ} = \begin{bmatrix} ð_{\flat}(q)(1,1) & 0 & 0 \\ 0 & ð_{\flat}(q)(2,2) & 0 \\ 0 & 0 & ð_{\flat}(q)(3,3) \end{bmatrix} \quad (17)$$

The algorithm is structured as follows:

Algorithm 1: The systematic algorithm utilizing the new formula of MDF
Input: Noise Images;
Output: estimate the value of b with the higher PNSR;
begin;
Input noise images;
Convoluted with the $3 * 3$ window;
Estimate the value of b with the higher PNSR;
end

At this point, we should mention that PNSR (peak signal-to-noise ratio) is a trade term for the ratio between a signal's utmost probable power and the strength of degrading noise, indicating its representation's accuracy. PSNR is usually expressed as a logarithmic number using the decibel scale since many images have a wide dynamic range. The structure has been formulated as follows:

$$\begin{aligned} PSNR &= 10 \cdot \log_{10}\left(\frac{\max(\Im)^2}{\Pi}\right) \\ &= 20 \cdot \log_{10}\left(\frac{\max(\Im)}{\sqrt{\Pi}}\right) \\ &= 20 \cdot \log_{10}(\max(\Im)) - 10 \cdot \log_{10}(\Pi) \end{aligned} \quad (18)$$

where max is the maximum value of the pixel and Π is the mean error

$$\Pi = \frac{1}{m\,n}\sum_{i=0}^{m-1}\sum_{j=0}^{n-1}[\Im(i,j) - \mathcal{T}(i,j)]^2,$$

Where $\mathcal{T}$ is the noise image.

Furthermore, the root-mean-square error (RMSE) is a commonly utilized ratio of the variations between standards predicted by a design, an estimator, and the principles discovered. The square root of the second model moment of the discrepancies between projected tenets and experimental ethics, or the quadratic mean of these alterations, is referred to as the RMSD. The following structure is used to identify it.

$$R = \sqrt{\frac{\sum_{j=1}^{n}(\hat{\Im}_j - \Im_j)^2}{n}}. \quad (19)$$

Each imaging unit (pixel) has a color value that can change when a photograph is compressed and subsequently uncompressed. Because signals have a wide dynamic range, PSNR (RMSD) is usually expressed in decibels, a logarithmic scale. The analysis is presented between PNSR (RMSD) and the probability of the pixel since the value of the pixel can be charged by its probability, as in this technique, which is based on the probability of the pixel (7) and (8).

5. Results and Discussion

In this part, the specified material from the previous part was used in this section to demonstrate the findings. Mathematica 11.2 was used to carry out the performance calculations. The two picture collections included two gray-scale images and two color images. The proposed method's windows mask designed to work with a 3 × 3 pixel window see Figures 3-5 Both PSNR and RMSD measurements were used to plan the MDF calculation presentations. PSNR values of $\flat$ in (7) and q for (8) are described in the intervals when $p \in (0,1)$ and $q \in (0,1)$.

The optimum value of PSNR is identified for the second approach, (8), for all proposed data, as shown in Table 1. The findings of the RMSD test are the same as those in Table 2. The author of the reference citemm6 utilized a one-dimensional fractal differential operator, which is compared to the recent technique. When compared to the findings of [6], it is evident that this solution provides a tremendous improvement. For example, in the earth image, the enhancement rate given by the PNSR test in [6] is equal to 89.99%, while the proposed method (7) yields 97.2% and (8) implies 92%.

Another description of MDF, based on specific special functions, might be proposed for further research. This approach may be used in various fields of computer science and can also be used to research different sorts of image processing. A range of applications or modifications is indicated using parametric mathematical frameworks. The effort of Ibrahim [6] is compared in the manner shown in Tables 1 and 2.

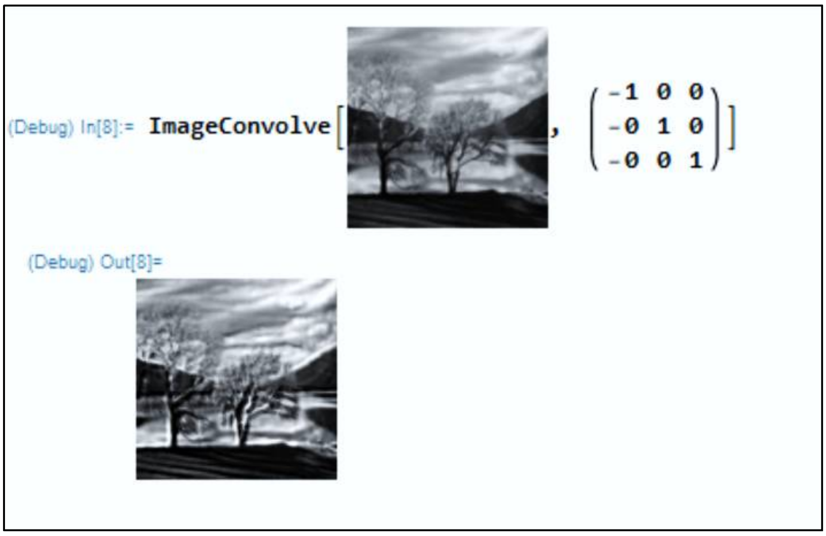

Figure 3: The convoluted image with the proposed windows $U_{135^{\circ}}$

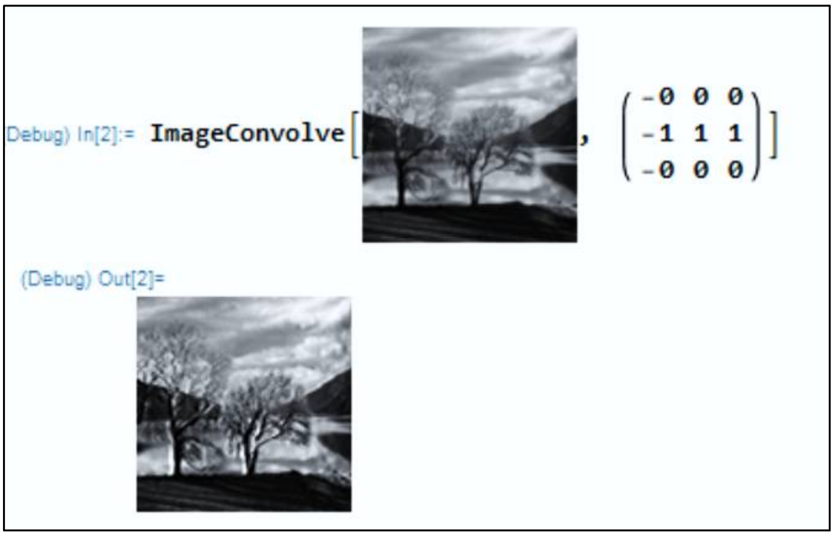

Figure 4: The image is proposed under the window $U_{0^{\circ}}$

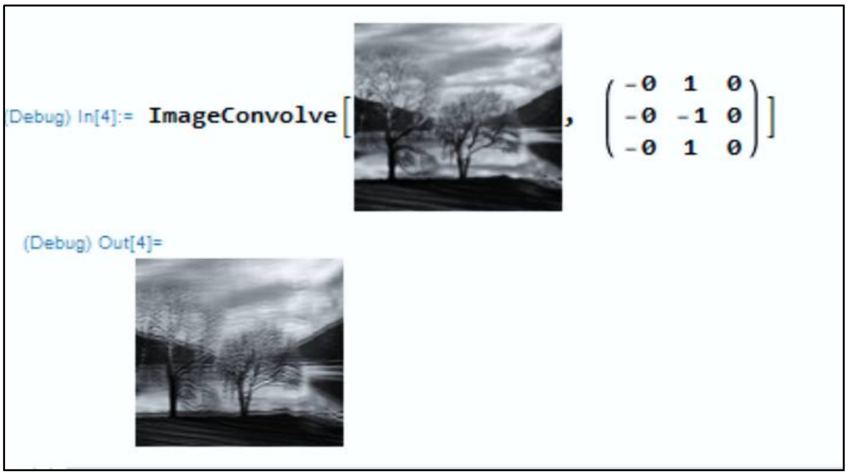

Figure 5: The image is the proposed under window $U_{90^{\circ}}$

Table 1: Table to new Multi-Dimensional Fractal (MDF)

Original image	MDF (7)	MDF (8)	Ibrahim [6]
			
35.4221	36.4396	38.6550	31.8798
			
21.9361	23.9712	25.3332	19.8885
	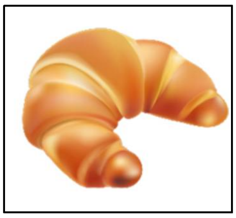	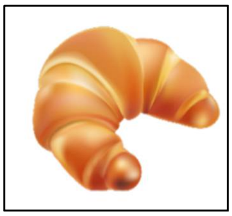	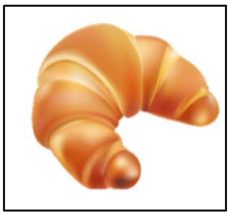
28.9911	30.0289	32.9378	27.2009
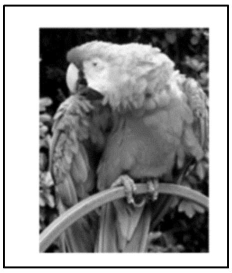			
24.4467	25.1489	27.6033	23.3020
			
26.1336	27.6974	30.0336	23.6602

Table 2: Table to test RMSD

Original image	**MDF (7)**	**MDF (8)**	**Ibrahim [6]**
			
14.1813	16.9559	18.7601	13.8832
			
25.0739	28.1358	32.1187	23.6665
			
23.1485	24.2946	26.7732	22.8992
			
14.9277	15.9246	17.9748	13.3943
			
20.3757	21.6333	23.6936	19.5277

6. Conclusions

A new method of image enhancement based on Multi-Dimensional Fractal (MDF) as a pre-processing step for low-contrast images is planned in this investigation. Different images with low gray-level have been enhanced by applying the suggested image enhancement model, which estimates the possibility of every image pixel. Regarding testing consequences on a diversity of images, the suggested approach outperforms existing approaches in the broad application of image development. The main restraint of this investigation is that the presentation of the suggested model extremely declines as the complexity of the input images grows. Future efforts may modify the existing model to detailed applications to optimize the elevation's aids. The improvement brought a 97% rate in PNSR in the earth image and a 95% rate in RMSD in the Lena image.

Author contribution

All authors contributed equally to this work.

Funding

This research received no specific grant from any funding agency in the public, commercial, or not-for-profit sectors.

Data availability statement

Not applicable.

Conflicts of interest

The authors of the current work do not have a conflict of interest.

References

[1] J. M Bioucas-Dias. and M. A. T. Figueiredo, Multiplicative noise removal using variable splitting and constrained optimization, IEEE Trans. Image Process., 19 (2010) 1720–1730. https://arxiv.org/abs/0912.1845v2.

[2] W.,Yao, Zhichang Guo, Jiebao Sun, Boying Wu, and Huijun Gao. Multiplicative Noise Removal for Texture Images Based on Adaptive Anisotropic Fractional Diffusion Equations, SIAM Journal on Imaging Sciences., 12 (2019) 839-873. https://doi.org/10.1137/18M1187192.

[3] J. Shi and S.Osher A nonlinear inverse scale space method for a convex multiplicative noise model, SIAM J. Imaging Sci., 1 (2008) 294–321. http://dx.doi.org/10.1137/070689954.

[4] Z. Zhou Zhichang Guo, Gang Dong, Jiebao Sun, Dazhi Zhang, and Boying WuA doubly degenerate diffusion model based on the gray level indicator for multiplicative noise removal, IEEE Trans. Image Process., 24 (2015) 249–260. http://dx.doi.org/10.1109/TIP.2014.2376185.

[5] J.Zhang and K.Chen "A total fractional-order variation model for image restoration with nonhomogeneous boundary conditions and its numerical solution", SIAM J. Imaging Sci., 8(2015)2487–2518.http://dx.doi.org/10.1155/2020/3714245.

[6] R. W. Ibrahim, A new image denoising model utilizing the conformable fractional calculus for multiplicative noise, SN Applied Sciences., 2 (2020) 1-11. https://doi.org/10.1007/s42452-019-1718-3.

[7] H. A. Jalab and R. W.Ibrahim Fractional Conway polynomials for image denoising with regularized fractional power parameters, J. Math. Imaging Vision., 51 (2015) 442–450. http://dx.doi.org/10.1007/s10851-014-0534-z.

[8] H. A. Jalab, and R. W. Ibrahim, Fractional Alexander polynomials for image denoising, Signal Process., 107 (2015) 340–354. http://dx.doi.org/10.1016/j.sigpro.2014.06.004.

[9] N. M.Al-Saidi, Shaimaa S. Al-Bundi, and Neseif J. Al-Jawari. A hybrid of fractal image coding and fractal dimension for an efficient retrieval method, Comput. Appl. Math., 37 (2018) 996-1011. https://doi.org/10.1007/S40314-016-0378-9.

[10] R. W. Ibrahim, Ali M. Hasan, and Hamid A. Jalab. A new deformable model based on fractional Wright energy function for tumor segmentation of volumetric brain MRI scans, Computer Methods and Programs in Biomedicine., 163 (2018) 21–28. http://dx.doi.org/10.1016/j.cmpb.2018.05.031.

[11] S. A.Yousif Hussam Y. Abdul-Wahed, and Nadia MG Al-Saidi. Extracting a new fractal and semi-variance attributes for texture images, AIP Conference Proceedings., 2183 (2019) 080006. http://dx.doi.org/10.1063/1.5136199.

[12] A. M.Hasan, Mohammed M. Al-Jawad, Hamid A. Jalab, Hadil Shaiba, Rabha W. Ibrahim, and Ala'A. R. AL-Shamasneh, Classification of Covid-19 coronavirus, pneumonia and healthy lungs in CT scans using Q-deformed entropy and deep learning features, Entropy., 22 (2020). http://dx.doi.org/10.3390/e22050517.

[13] N. S. Hee , J. Y. Choi , A method of image enhancement and fractal dimension for detection of microcalcifications in mammogram, In Proceedings of the 20th Annual International Conference of the IEEE Engineering in Medicine and Biology Society, Vol. 20, Biomedical Engineering Towards the Year 2000 and Beyond (Cat. No. 98CH36286)., 2(1998) 1009-1012. http://dx.doi.org/10.1109/IEMBS.1998.745620.

[14] C.Ting, W. Wang, S. Tighe, S. Wang, Crack image detection based on fractional differential and fractal dimension, IET Comput. Vision, 13 (2019) 79-85. https://doi.org/10.1049/iet-cvi.2018.5337.

[15] G-B. So, H-R. So, G-G. Jin, Enhancement of the box-counting algorithm for fractal dimension estimation, Pattern Recognit. Lett., 98 (2017) 53-58. https://doi.org/10.1016/j.patrec.2017.08.022

[16] L. Lihua, D. Zhang, Y. Tian, X.i Zhou,Sound-Absorption Performance and Fractal Dimension Feature of Kapok Fibre/Polycaprolactone Composites, Coatings, 11 (2021)1000. http://dx.doi.org/10.3390/coatings11081000.

[17] R. J.Al-Azawi, N. M. Al-Saidi, H. A. Jalab, H.Kahtan, R. W. Ibrahim, Efficient classification of COVID-19 CT scans by using q-transform model for feature extraction, PeerJ Comput. Sci., 7 (2021) e553. http://dx.doi.org/10.7717/peerj-cs.553.

[18] H. A.Jalab, R.W. Ibrahim, A. M. Hasan, F. K. Karim, A. R. Al-Shamasneh, D. Baleanu, A New medical image enhancement algorithm based on fractional calculus, CMC-Comput. Mater. Continua , 68 (2021) 1467-1483. http://dx.doi.org/10.32604/cmc.2021.016047.

[19] R. J.Al-Azawi, N. M. Al-Saidi, H. A. Jalab, R.W. Ibrahim, Dumitru Baleanu , Image splicing detection based on texture features with fractal entropy, CMC-Comput. Mater. Continua, 69 (2021) 3903-3915.http://dx.doi.org/10.32604/cmc.2021.020368.

[20] Petrou M. Image Processing: The Fundamentals, John Wiley & Sons, 2010.

[21] L.Yun, J.Shu , Fractal dimension of random attractors for non-autonomous fractional stochastic Ginzburg–Landau equations with multiplicative noise, Dyn. Syst. Int. J., 34 (2019) 274-300. http://dx.doi.org/10.1080/14689367.2018.1523368.

[22] N. M. G. Al-Saidi, Password authentication based on fractal coding scheme, J. Appl. Math., 2012 (2012) 1-16. https://doi.org/10.1155/2012/340861

[23] N.M.G. Al-Saidi, M.R.M. Said,Biometric identification based local iterated function systems, Eur.Phys. J. Spec. Top., 223 (2014) 1647-1662. http://dx.doi.org/10.1140/epjst/e2014-02120-4

[24] T.Sun, X. Wang, D. Lin , R. Bao , D.Jiang , B. Ding , D. Li, Medical image security authentication method based on wavelet reconstruction and fractal dimension, Int. J. Distrib. Sens. Netw., 17 (2021)1-9. http://dx.doi.org/10.1177/15501477211014132.

[25] Mandelbrot,B. B. The fractal geometry of nature. New York: WH freeman, 1982.

[26] M. Kruk, B. Świderski, S .Osowski, Box-counting fractal dimension in application to recognition of hypertension through the retinal image analysis, dimension, 89 (2013) 286- 289 .

[27] F. Huang, B.Dashtbozorg, J.Zhang, E. Bekkers, S. Abbasi-Sureshjani, T. T. J. M. Berendschot, B. M. ter Haar Romeny,Reliability of using retinal vascular fractal dimension as a biomarker in the diabetic retinopathy detection, J. Ophthalmol., 2016 (2016)13. https://doi.org/10.1155/2016/6259047

[28] S. Dinesena et al., Retinal Vascular Fractal Dimensions and Their Association with Macrovascular Cardiac Disease, Ophthalmic Res., 64 (2021) 561–566. https://doi.org/10.1159/000514442

[29] R.Alfred, On the dimension and entropy of probability distributions, Acta Mathematica Academiae Scientiarum Hungarica,10 (1959) 193-215. https://doi.org/10.1007/BF02063299

[30] Tey, Kai Yuan, Kelvin Teo, Anna Tan, Kavya Devarajan, Bingyao Tan, Jacqueline Tan, Leopold Schmetterer, MAng, Optical coherence tomography angiography in diabetic retinopathy: a review of current applications,Eye and Vision,6 (2019) 1-10. http://dx.doi.org/10.1186/s40662-019-0160-3

[31] T. Stefan, Multifractal geometry in analysis and processing of digital retinal photographs for early diagnosis of human diabetic macular edema, Curr. Eye Res., 38 (2013) 781-792. http://dx.doi.org/10.3109/02713683.2013.779722

[32] Ott, E. Chaos in Dynamical Systems, Cambridge University Press: Cambridge, UK; New York, NY, USA, 1993.

[33] S.Yu, L. Vasudevan, Fractal Dimension and Retinal Pathology: A Meta-Analysis, Appl. Sci., 11 (2021) 2376. https://doi.org/10.3390/app11052376

[34] T.Alberti, R. V. Donner, S.Vannitsem, Multiscale fractal dimension analysis of a reduced order model of coupled ocean-atmosphere dynamics, Earth Syst. Dyn., 12 (2021) 837–855. http://dx.doi.org/10.5194/esd-12-837-2021

[35] M. C., Jones, H. W. Lotwick, On the errors involved in computing the empirical characteristic function , J. Stat. Comput. Simul.,17 (1983) 133-149. https://doi.org/10.1080/00949658308810650

[36] D. L. Donoho, J. M. Johnstone, Ideal spatial adaptation by wavelet shrinkage, biometrika, 81 (1994) 425-455.https://doi.org/10.2307/2337118

[37] S. Dong-Hyuk, et al., Block-based noise estimation using adaptive Gaussian filtering, IEEE Trans. Consum. Electron., 51 (2005) 218-226. https://doi.org/10.1109/TCE.2005.1405723

[38] L.Wei, and W.LinAdditive white Gaussian noise level estimation in SVD domain for images, IEEE Trans. Image Process., 22 (2012) 872-883. http://dx.doi.org/10.1109/TIP.2012.2219544

[39] Fan, Linwei, Fan Zhang, Hui Fan, and Caiming Zhang. Brief review of image denoising techniques , Vis. Comput. Ind. Biomed. Art, 2 (2019) 1-12. https://doi.org/10.1186/s42492-019-0016-7

[40] A. Boukharouba, Smoothed Rectangular Function-Based FIR Filter Design, Circuits Syst. Signal Process., 36 (2017) 4756-4767. https://doi.org/10.1007/s00034-017-0529-2

[41] J.Yang, W. B., Ronald , L. R. Steven ,Applying image processing methods to study hydrodynamic characteristics in a rectangular spouted bed, Chem. Eng. Sci., 188 (2018) 238-251. https://doi.org/10.1016/j.ces.2018.05.057

[42] L.Bargsten , S.Alexander, SpeckleGAN: a generative adversarial network with an adaptive speckle layer to augment limited training data for ultrasound image processing, Int. J. Comput. Assisted Radiol. Surg., 15 (2020) 1427-1436. http://dx.doi.org/10.1007/s11548-020-02203-1

[43] Y-B. He, Y-J. Zeng, H-X. Chen, S-X. Xiao, Y-W. Wang, S-Y, Huang,Research on improved edge extraction algorithm of rectangular piece, Int. J. Mod. Phys. C., 25 (2018) 1850007.https://doi.org/10.1142/S0129183118500079

[44] Q-X. Meng, W-Y. Xu, H-L. Wang, X-Y. Zhuang, W-C. Xie, T. Rabczuk, DigiSim—an open source software package for heterogeneous material modeling based on digital image processing, Adv. Eng. Software, 148 (2020) 102836. http://dx.doi.org/10.1016/j.advengsoft.2020.102836

[45] F. Ferreira, I.M Pires, M .Costa, V. Ponciano, N.M Garcia ,A Systematic Investigation of Models for Color Image Processing in Wound Size Estimation, Computers,10 (2021) 43. https://doi.org/10.3390/computers10040043

[46] J. Chen, K. Chen, H. Chen, Z. Zou, Z. Shi, A Degraded Reconstruction Enhancement-based Method for Tiny Ship Detection in Remote Sensing Images with A New Large-scale Dataset, IEEE Trans. Geosci. Remote Sens., 60(2022) 1-14. http://dx.doi.org/10.1109/TGRS.2022.3180894

[47] M. Sunouchi, M. Yoshioka, Diversity-Robust Acoustic Feature Signatures Based on Multiscale Fractal Dimension for Similarity Search of Environmental Sounds, IEICE Trans. Inf. Syst., 104 (2021) 1734-1748. https://doi.org/10.1587/transinf.2021EDP7016

[48] V. Muneeswaran, P. Nagaraj, K. Puneeth Sai, E. Ajay Kumar, S. Reddy Chanakya, Enhanced image compression using fractal and tree seed-bio inspired algorithm, In Second Int. Conf. Electron. Sustainable Commun. Syst., Coimbatore, India, 2021, 1125-1130.https://doi.org/10.1109/ICESC51422.2021.9532850

[49] A. Ganesan, S.M .Santhanam, Fractal adaptive weight synthesized–local directional pattern–based image classification using enhanced tree seed algorithm, Environ. Sci. Pollut. Res.,29 (2022) 77462–77481. https://doi.org/10.1007/s11356-022-20265-3

[50] H. Liang, M. Tsuei, N. Abbott, F. You, AI Framework with Computational Box Counting and Integer Programming Removes Quantization Error in Fractal Dimension Analysis of Optical Images, Chem. Eng. J., 446 (2022) 137058. http://dx.doi.org/10.1016/j.cej.2022.137058